Environ. Sci. Technol. **1999**, *33,* 3749−3754

Kinetics of Mixed Ni−Al Precipitate Formation on a Soil Clay Fraction

DARRYL R. ROBERTS,*,† ANDRÉ M. SCHEIDEGGER,‡ AND DONALD L. SPARKS†

Department of Plant and Soil Sciences, University of Delaware, 147 Townsend Hall, Newark, Delaware 19717-1303, and Waste Management Laboratory, Paul Scherrer Institute, CH-5232 Villigen PSI, Switzerland

The kinetics of mixed Ni−Al layered double hydroxide (LDH) precipitate formation on a soil clay fraction was monitored using X-ray absorption fine structure (XAFS) spectroscopy. The kinetic behavior was monitored at pH 6.0, 6.8, and 7.5 in order to determine the effect of reaction pH on precipitate formation. XAFS analyses were performed on a Ni-reacted whole soil at pH 7.5 to determine the effect of metal oxides and organic matter on mixed Ni−Al LDH formation. The initial Ni concentration was 3 mM with a solid/solution ratio of 10 g L^{-1} in 0.1 M $NaNO_3$. Initial Ni sorption kinetics on the soil clay were rapid at all pH values but differed at each pH for longer reaction times. The sorption kinetics at pH 7.5 were characterized by an extremely rapid initial step with nearly 75% of Ni sorbed within 20 h, followed by a slower step with nearly 100% of the Ni removed from solution within 150 h. XAFS analysis of the pH 7.5 sorption samples indicated the formation of a mixed Ni−Al LDH within 15 min. The sorption kinetics at pH 6.8 were initially rapid, followed by a slow step, and XAFS revealed the formation of a Ni−Al LDH within 2 h. At pH 6.0, Ni sorption did not exceed 20%, and XAFS analysis revealed no LDH formation within 72 h. XAFS analysis for the whole soil indicated a mixed Ni−Al phase formed at pH 7.5 after 24 h of reaction. These findings indicate that mixed metal precipitate formation occurs in heterogeneous clay systems and whole soils; therefore, they should be considered when predicting and modeling the fate of metals in subsurface environments.

Introduction

Contamination of surface and subsurface environments by heavy metals has established the need to understand metal−soil interactions. Heavy metals may enter soil and aquatic environments via sewage sludge application, mine waste, industrial waste disposal, atmospheric deposition, and application of fertilizers and pesticides (*1*). It is imperative to understand the sorption mechanisms by which metals such as As, Cd, Cr, Cu, Ni, or Pb partition to soil and soil components to aid in the development of remediation strategies and the formulation of models designed to predict the fate and mobility of contaminant metals.

Macroscopic studies have been performed to determine the effect of ionic strength, initial metal concentration, pH, solid/solution ratio, and competing ligands on the sorption of metals to soils, clay minerals, and metal oxides. (*2*−*6*). While such macroscopic approaches are valuable in characterizing sorption behavior, they cannot elucidate molecular reactions (*7*). In recent years, the application of advanced spectroscopic and microscopic tools has helped define the mechanisms controlling contaminant reactions in soils and aquatic environments (*8, 9*). X-ray absorption fine structure (XAFS) spectroscopy has been a valuable tool to characterize sorption mechanisms of metals sorbed to single-component metal oxides and reference clay minerals (*10*−*20*) and to determine the speciation of contaminants in soils (*21*−*24*).

Recent XAFS studies have shown the formation of precipitates during metal sorption to mineral and oxide surfaces over rapid time scales, at pH levels undersaturated with respect to pure metal hydroxide solubility, and at metal surface coverages below a theoretical monolayer coverage (*10, 11, 14, 16, 19, 25*−*29*). For example, Scheidegger et al. (*27*) used XAFS to discern the local atomic structure of Ni sorbed on pyrophyllite (an Al-bearing 2:1 clay mineral). They observed the presence of a mixed Ni−Al hydroxide phase at low surface loading and at reaction conditions undersaturated with respect to the formation of $Ni(OH)_2$(s). Towle et al. (*19*) demonstrated that Co sorption on Al_2O_3 resulted in the formation of a layered double hydroxide (LDH) phase containing both Co and substrate-derived Al ions from solutions undersaturated with respect to a pure cobalt hydroxide. Precipitate phases may also form in the presence of non-Al-bearing minerals as demonstrated in a study by Scheinost et al. (*30*). Using diffuse reflectance spectroscopy (DRS), they showed that α-$Ni(OH)_2$ formed upon Ni sorption to both talc and silica. The above studies demonstrate that the sorbent may determine the structure of the metal precipitate phase that forms upon metal sorption.

While the previously mentioned metal sorption studies have established that metal hydroxide precipitates may form on model clay minerals and synthesized oxides under specific reaction conditions, the results are difficult to apply to soil environments where multiple clay minerals are present and a range of pH values may occur. In addition, soil systems are rarely, if ever, at equilibrium, making it important to study metal sorption reactions over a range of reaction times (*31*). Characterizing metal sorption mechanisms on soils and sediments using XAFS spectroscopy has proven difficult since heterogeneous sorbents possess a broad array of sorption sites, each possessing a unique spectroscopic signature (*24*). Isolating specific fractions of whole soils for metal sorption studies may reduce such complications.

To determine the likelihood of metal precipitate formation in soils, the sorbent phase should be heterogeneous in order to simulate a soil environment while also being fully characterized to ease in the application of an analytical technique such as XAFS. Since in many soils the most reactive mineral sites for sorption are present in the <2-μm size fraction, this fraction is a good model for studying sorption processes in whole soils. Accordingly, our approach was to make the progression from previous studies using model clay minerals to a soil clay mineral fraction and finally to provide limited data for a whole soil. The majority of the results presented here concentrate on the clay mineral fraction as this system is well-characterized and provides a strong case to compare whole soils, which we are investigating in more detail. The objective of this study was to determine if metal hydroxide precipitates form upon Ni sorption to a well-characterized soil clay fraction and the whole soil from which the clay was derived. The <2-mm fraction of a whole

* Corresponding author e-mail: droberts@udel.edu; phone: (302)-831-1595; fax: (302)831-0605.
† University of Delaware.
‡ Paul Scherrer Institute.

10.1021/es990235e CCC: $18.00
Published on Web 09/23/1999

soil and the <2-μm size fraction treated to remove organic matter and metal oxides were used in the study. The sorption of Ni over a range of pH and reaction times was monitored using XAFS to determine the influence of these variables on mixed metal precipitate formation. This information will be valuable in assessing whether metal precipitate formation is likely to occur in heterogeneous soil systems and to characterize the type of precipitate phase formed (layered double hydroxide vs metal hydroxide).

Experimental Methods

Materials. The soil used in this study was the Ap horizon of a Matapeake silt loam (Typic-Hapludult). For the whole soil experiments the <2-mm fraction was isolated. For the clay fraction experiments, a series of treatment steps were used to isolate the <2-μm fraction. Organic matter was removed by treatment with 4−6% NaOCl adjusted to pH 9.5 at a temperature of 70 °C (*32*). Next, free iron and aluminum oxides were extracted using the sodium dithionite−citrate−bicarbonate method (*33*). The <2-μm size fraction was separated by centrifugation and decantation. The clay fraction was then Na-saturated by washing three times with 1.0 M NaCl followed by dialysis in deionized−distilled (DDI) water to remove excess salts. The clay fraction was then freeze-dried prior to characterization. The purification procedures of the whole soil resulted in a relatively pure mixture of aluminosilicate clay minerals from the collected <2-μm fraction.

The mineral suite of the soil, as determined by X-ray diffraction (XRD) using oriented slide mounts, was aluminum hydroxy interlayered vermiculite (HIV) ≥ kaolinite ≫ mica. Minor amounts of gibbsite and quartz were also present (*34*). Thermal gravimetric analysis (TGA) and differential scanning calorimetry (DSC) indicated slightly more HIV than kaolinite (*35*). The total surface area of the <2-mm fraction, as determined by EGME, was 15.5 $m^2\ g^{-1}$ The total surface area of the <2-μm fraction, as determined by EGME, was 96.7 $m^2\ g^{-1}$, and the external surface area, as determined by BET-N_2 analysis, was 41.1 $m^2\ g^{-1}$ (*36*). The CEC of the clay as determined by Ca/Mg exchange at pH 6.5 was 60.5 $cmol_c\ kg^{-1}$ (*37*).

Macroscopic Sorption Kinetics. Four separate reaction vessels were used to study the influence of pH on the rate of Ni sorption to the soil clay fraction and whole soil. Prior to initializing Ni sorption, the solids were hydrated for 24 h by suspending ~5 g of soil clay or soil in 500 mL of 0.1 M $NaNO_3$ solution adjusted to pH 6.0, 6.8, or 7.5 using either 0.1 M HNO_3 or 0.1 M NaOH. For the whole soil study, only pH 7.5 was selected to ensure sufficient metal loading and a strong XAFS signal as the heterogeneity of the soil could potentially result in a high level of spectral noise. After hydration of the clay or soil, Ni from a 0.1 M $Ni(NO_3)_2$ stock solution was added in 1-mL aliquots to achieve initial conditions of $[Ni]_0 = 3$ mM, $I = 0.1$ M, and a solid/solution ratio = 10 g L^{-1}.

The initial Ni concentration of 3 mM was selected to directly compare this study to the work of Scheidegger et al. (*20*). Mattigod et al. (*38*) extensively studied the solubility of crystalline $Ni(OH)_2$ over a range of pH values and reaction times. Their results verify that under the reaction conditions similar to those found in our study (pH = 7.5, $[Ni]_0 = 3$ mM), the solution was undersaturated with respect to $Ni(OH)_2$. Therefore we are confident the 3 mM $[Ni]_0$ was below the concentration required for the formation of $Ni(OH)_2$ in solution at all pH values used in this study; therefore, the removal of Ni from solution was not due to the formation of $Ni(OH)_2$. Solubility data for mixed Ni−Al hydroxides is lacking in the literature and is therefore an area in need of investigation. Thompson et al. (*39*) showed that cobalt hydrotalcites were the dominant stable phase at near-neutral pH values as compared to cobalt hydroxide precipitates. Only above a certain threshold pH (>7.5) was cobalt hydroxide a stable precipitate. They concluded that the availability of Al seemed to be a major factor in whether a cobalt hydrotalcite phase or a cobalt hydroxide phase formed. Similarly, we would expect a Ni−Al layered double hydroxide phase to be more stable than a $Ni(OH)_2$ precipitate under the reaction conditions studied here, although sufficient data are lacking to fully support this hypothesis.

During the first 48 h of sorption, the pH was held constant at 6.0, 6.8, or 7.5 by automatic titration with 0.1 M NaOH or 0.1 M HNO_3 using a pH-stat apparatus. The suspension was stirred at 350 rpm with a Teflon stir bar, the temperature was maintained at 25 °C using a water bath, and the vessels were purged with N_2 to eliminate CO_2. After 48 h, the vessels were placed on an orbital shaker operating at a speed of 150 orbits min^{-1}, and the pH was adjusted daily with either 0.1 M NaOH or 0.1 M HNO_3. For reaction times up to 700 h, 5-mL subsamples were transferred to centrifuge tubes and centrifuged at 12 000 rpm for 4 min. The supernatant was filtered through a 0.2-μm membrane filter and analyzed for dissolved Ni by inductively coupled plasma emission spectrometry (ICP). The amount of sorbed Ni was calculated as the difference between the initial and final Ni concentration in solution. For XAFS analysis, solids were isolated from 40-mL aliquots. The solids were washed with 40 mL of DDI water to remove entrained solution. Insignificant quantities of sorbed Ni were removed from the soil clay by this washing procedure. Short-term samples (15 min−2 h) for XAFS analysis were prepared at the beamline to avoid possible storage effects.

XAFS Analysis. XAFS spectra were collected for the Ni-reacted clay and soil samples at beamline X-11A at the National Synchrotron Light Source (NSLS) at Brookhaven National Laboratory, Upton, NY. The electron beam energy was 2.5 GeV with a beam current between 120 and 240 mA. The monochromator consisted of two parallel Si(111) crystals with an entrance slit width of 0.5 mm. Higher order harmonics were removed by detuning I_o by 25% at the Ni K-edge (8333 eV). The samples were placed in Al holders and held in place with Kapton tape. Samples were kept at 77 K with a coldfinger to reduce dampening of the XAFS oscillation by thermal disorder (*27*). Studies in our laboratory indicate no differences in structural information derived from collecting XAFS spectra at room temperature as compared to collection at 77 K. Interference from the Cu coldfinger was eliminated by covering the exposed portions with Pb foil. The data were collected in fluorescence mode using a Stern-Heald type detector filled with Ar and equipped with a Co-3μm filter (*40*).

The data analysis program MacXAFS was used for background subtraction and Fourier filtering of the XAFS data (*41*). Three scans were averaged for each sample, and the energy position was normalized relative to E_o for Ni metal. The position of E_o within sample spectra was assigned to the maximum of the derivative. The χ function was extracted from the raw data using a linear preedge background and a spline postedge background. The data were then converted from energy to k space. The χ functions were weighted by k^3 in order to compensate for dampening of the XAFS amplitude with increasing k. The data were then Fourier transformed (Δk = 3.2−14 $Å^{-1}$) to yield a radial structure function (RSF).

The k^3-weighted spectra were fit in k space using XFTools included in MacXAFS (*42*). Single-shell data and phase shifts for Ni−Ni, Ni−O, and Ni−Al backscatterers were generated using FEFF 6.0 (*43*). The input file was created with the program ATOMS using the β-$Ni(OH)_2$ structure with two of the Ni atoms at 3.117 Å replaced by Al (*44*). The theoretical spectra were Fourier filtered over ranges identical to those

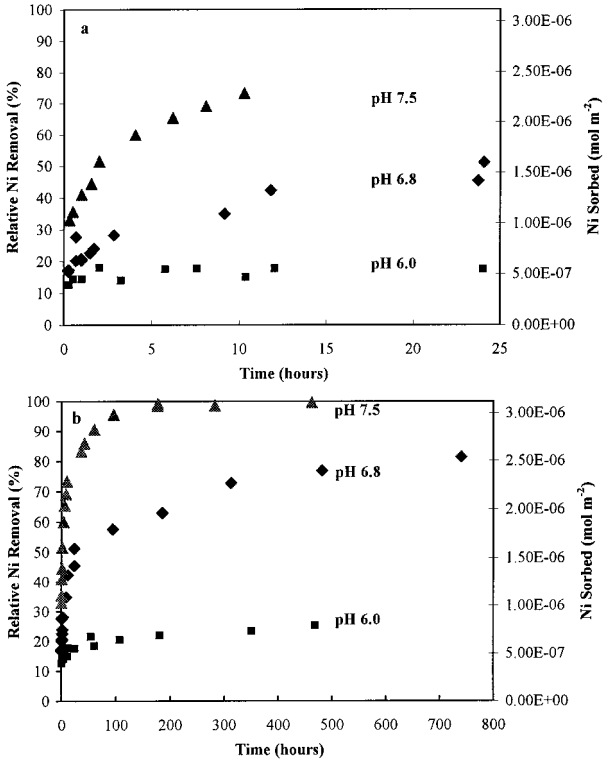

FIGURE 1. Ni sorption kinetics on soil clay at pH 6.0, 6.8, and 7.5, I = 0.1 M $NaNO_3$, $[Ni]_0$ = 3 mM, solid/solution = 10 g/L. (a) Ni sorption within 25 h. (b) Ni sorption over entire reaction period.

used in the fits (*20*). Multi-shell *k* space fits were performed over a *k* range of 3.2−14 Å and an *R* range of 1.07−3.12 Å. For the Ni-reacted samples, the Debye−Waller factors for the Ni−Ni and Ni−Al shells were fixed at 0.005. This value has previously been used to fit hydroxide precipitates containing both Ni−Al and Co−Al bonds (*19, 20, 45*). In addition, the Ni−Ni and Ni−Al bond distances were constrained to be equal during the fitting process. These constraints reduced the number of free parameters to 8. A single edge shift (ΔE_o) was minimized for all shells during the curve-fitting procedure.

The errors in the fitting were estimated based on the findings of other researchers investigating systems with similar metal hydroxide formation (*20, 26, 46*). For example, Scheidegger et al. (*20*) compared XAFS-derived structural parameters of a Ni−Al coprecipitate with parameters derived by XRD. They found R_{Ni-O} and R_{Ni-Ni} to be accurate to ±0.020 Å, the N_{Ni-O} and N_{Ni-Ni} values to be accurate to ±20%, the N_{Ni-Al} ± 60%, and R_{Ni-Al} ± 0.06 Å. These error estimates were applied to this research.

Results and Discussion

Ni Sorption Kinetics. The time dependence of Ni sorption at pH 6.0, 6.8, and 7.5 on the soil clay fraction is shown in Figure 1. An initial rapid uptake occurred at all pH values. However, after several hours the rate of sorption at the various pH values differed. At any given time, the Ni loading level increased with increasing pH. Figure 1a shows Ni sorption within 25 h at each pH value, while Figure 1b shows Ni sorption over the entire reaction period. At pH 6.0, 10% of the initial Ni was sorbed in less than 1 h, and this value increased to 20% within 500 h. Although this is a large relative increase, the total amount removed is small as compared to sorption at pH 6.8 and pH 7.5. At pH 6.8, the Ni sorption proceeded quite rapidly initially with 40% of the initial Ni sorbed in 10 h, followed by a more gradual sorption period in which 80% of the initial Ni was sorbed within 800 h. The

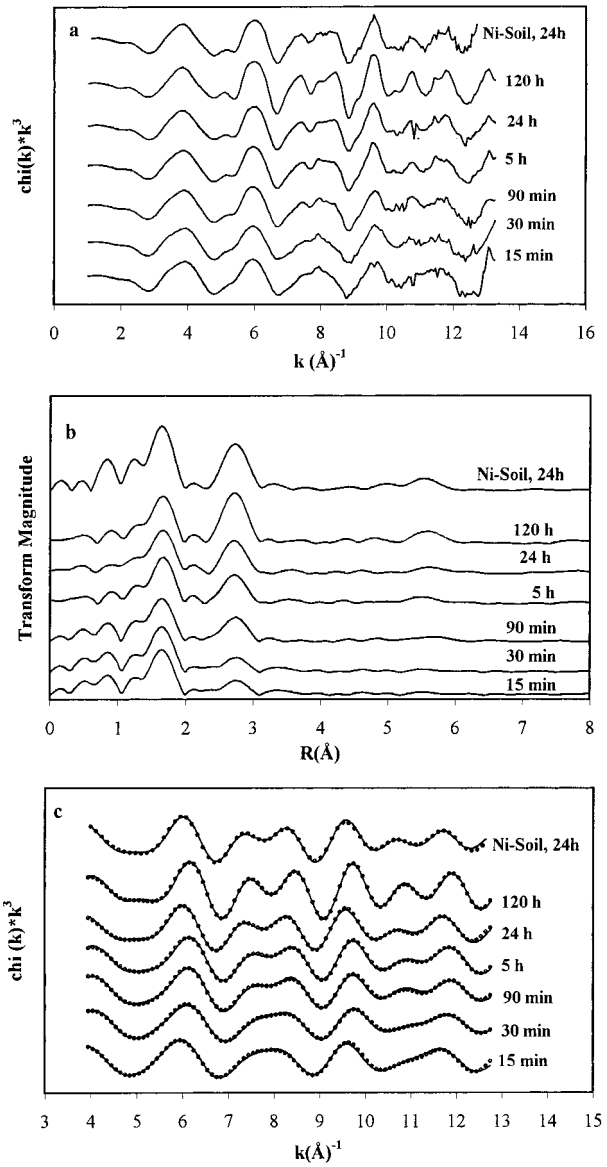

FIGURE 2. Results of EXAFS experiments performed at pH 7.5. (a) k^3-weighted, normalized, background-subtracted χ functions for Ni sorbed on soil clay for different times and whole soil. (b) Fourier transforms of χ functions in panel a, uncorrected for phase shift. (c) Experimental k^3-weighted XAFS data (solid line) of Fourier back-transformed spectra in comparison to theoretical spectra (dotted line) using multi-shell least-squares fitting.

kinetics at pH 7.5 were characterized by an extremely rapid initial step with nearly 75% of Ni sorbed after 12 h, followed by a much slower sorption region where nearly 100% of the Ni was removed from solution within 200 h.

XAFS Analyses of Ni-Reacted Clay and Soil at pH 7.5. The k^3-weighted, normalized, background-subtracted χ functions for Ni sorbed on the soil clay and whole soil at pH 7.5 for different times are presented in Figure 2a. For the soil clay samples, as reaction time increased from 10 min to 120 h, the amount of Ni on the clay mineral surface increased leading to more pronounced oscillations in the XAFS signal at higher energies (>8 $Å^{-1}$). At short reaction times (15−90 min), spectral noise was more pronounced due to a lower Ni loading on the surface. The spectrum for the Ni-reacted whole soil after 24 h has a similar beat pattern to the 24-h soil clay sample, although with slightly more noise. The truncated feature seen in all the spectra at ~8 $Å^{-1}$ has been shown to be a unique fingerprint of Ni−Al layered double

TABLE 1. Structural Parameters of Ni Sorbed on Soil Clay and Whole Soil and Parameters for Reference Ni-Containing Phases

	first shell			second shell					
	Ni−O			Ni−Ni			Ni−Al		
	R (Å)[a,d]	N[b,e]	$\Delta\sigma^2$ (Å^2)[c,e]	R (Å)[d,i]	N[e]	$\Delta\sigma^2$ (Å^2)[e,h]	R (Å)[f,i]	N[g]	$\Delta\sigma^2$ (Å^2)[e,h]
				pH 7.5					
15 min	2.06	5.7	0.0027	3.05	0.8	0.005	3.05	0.9	0.005
30 min	2.05	6.0	0.0040	3.05	1.7	0.005	3.05	1.2	0.005
90 min	2.05	6.9	0.0054	3.06	2.5	0.005	3.06	0.8	0.005
5 h	2.05	5.4	0.0030	3.06	3.4	0.005	3.06	1.5	0.005
24 h	2.05	5.2	0.0028	3.06	4.0	0.005	3.06	1.1	0.005
120 h	2.05	5.8	0.0034	3.05	5.6	0.005	3.05	1.8	0.005
soil, 24 h	2.05	5.9	0.0031	3.06	3.4	0.005	3.06	0.7	0.005
				pH 6.8					
15 min	2.05	5.9	0.0032						
2 h	2.05	5.7	0.0033	3.05	1.6	0.0050	3.05	0.9	0.005
72 h	2.05	5.4	0.0028	3.04	3.3	0.0050	3.04	1.6	0.005
				pH 6.0					
2 h	2.05	5.6	0.0052						
72 h	2.06	5.7	0.0046						
				References[j]					
α-Ni(OH)$_2$	2.03	5.1	0.0055	3.08	5.1	0.0079			
Ni−Al LDH	2.05	6.5	0.0073	3.06	4.8	0.0078	3.06	1.4	0.0078

[a] Interatomic distance. [b] Coordination number. [c] Debye−Waller factor. Fit quality estimated accuracy: [d] ±0.02 Å. [e] ±20%. [f] ±0.06 Å. [g] ±60%. [h] Debye−Waller factors were fixed at 0.005 Å^2. [i] Ni−Ni and Ni−Al distances constrained to be equal during fitting. [j] d'Espinose de la Caillerie et al., 1995 (*26*).

hydroxides, distinguishable from a Ni hydroxide precipitate (*47*). The spectra were Fourier transformed to produce the radial structure functions shown in Figure 2b. These spectra are uncorrected for phase shift. The first peak at $R \cong 1.7$ Å represents the first coordination shell of Ni and remains relatively constant in amplitude and position with increasing reaction time. A second peak at $R \cong 2.8$ Å appears within 15 min for the soil clay samples and continuously increases in magnitude within 120 h. This peak is likely due to contributions from second nearest Ni and/or Ni−Al neighbors around the central absorber. The same peaks are present in the Ni-reacted untreated whole soil sample. The second shell of the RSFs indicates that some type of Ni precipitate is forming in both the soil clay and whole soil samples and continuing to grow over time.

Comparison of the k^3-weighted XAFS functions for the Fourier back-transformed spectra to the theoretical spectra derived by fitting theoretical Ni−O, Ni−Ni, and Ni−Al scattering paths to the raw data is shown in Figure 2c. The comparison indicates that the theoretical paths provide a good representation of the experimental data. The structural parameters derived from the fits are presented in Table 1. Analysis shows that the first shell is consistent with Ni surrounded by ∼6 O atoms, indicating that Ni is in an octahedral coordination environment. The Ni−O bond distance (R_{Ni-O}) is approximately 2.05 Å in all samples, and the coordination number (N) essentially remains constant with time. Analysis of the second shell indicates the presence of a second-neighbor Ni atom around the central absorber at a bond distance ∼3.05 Å. Al was included in fitting the second shell based on studies by Scheinost et al. (*30*) investigating Ni sorption on Al-bearing and non-Al-bearing metal oxides and reference clay minerals. Using DRS, they showed that if Al was present in the sorbent structure (pyrophyllite, gibbsite), a Ni−Al LDH formed. In contrast, Ni sorption to non-Al-bearing minerals (talc, silica) resulted in the formation of α-Ni(OH)$_2$ absent of any Al. Since the clay fraction and whole soil contain potential sources of soluble Al (kaolinite, Al−HIV, gibbsite), we assumed that Al was incorporated into the metal precipitates that formed. The fitting results supported this initial assumption. The N_{Ni-Ni} increased from 0.8 after 15 min to 5.6 after a reaction time of 120 h. These results show that formation of a precipitate was occurring within 15 min at pH 7.5 for the soil clay fraction. For the whole soil, a similar precipitate formed within 24 h. The Ni−Ni bond distance in the clay and soil samples resembles the Ni−Ni bond distance in a Ni−Al LDH phase (*26*). For both Ni−Al LDH and our sorption samples, the Ni−Ni bond distance (R = 3.05−3.06 Å) is shorter than the Ni−Ni bond in α-Ni(OH)$_2$ (R = 3.08 Å) (*26*). This indicates that a mixed Ni−Al layered double hydroxide is forming upon Ni sorption to the soil clay fraction and the whole soil. On the basis of the results for the whole soil, the presence of organic matter and metal oxides did not inhibit the formation of a mixed Ni−Al LDH phase. Under the reaction conditions studied in this experiment, the formation of mixed metal precipitates in soil environments is a viable metal sorption mechanism. Further studies to investigate the formation of these phases in soils are currently underway.

The XAFS results obtained in this study closely resemble the findings of Scheidegger et al. (*20*) for Ni sorption on specimen clay minerals and aluminum hydroxide. The formation of precipitates was observed in the presence of pyrophyllite, kaolinite, gibbsite, and montmorillonite at pH 7.5. The precipitate was identified as a mixed Ni−Al LDH by XAFS spectroscopy. It was hypothesized that coprecipitated Al was derived from the sorbent structure. While the sorbents in our experiment was more heterogeneous and complex in nature than the sorbents used in the study by Scheidegger et al., the XAFS data indicate that a precipitate phase formed within 15 min. Other sorption processes may be occurring concurrently with precipitation as the soil clay has Al−OH and Si−OH sites as well as permanent-charge sites where Ni can potentially be sorbed as inner-sphere and outer-sphere complexes, respectively. Using our XAFS data, we were not able to distinguish between adsorbed Ni and Ni incorporated into a precipitate phase. However, the growth of the Ni−Ni peak over time (Table 1) indicates that precipitate formation is an important mechanism in early reaction times and dominates Ni uptake at longer reaction times.

XAFS Analyses of Ni-Reacted Clay at pH 6.8. The k^3-weighted, normalized, background-subtracted χ functions for Ni sorbed on the soil clay at pH 6.8 for different times are shown in Figure 3a. With increasing reaction time (15 min−

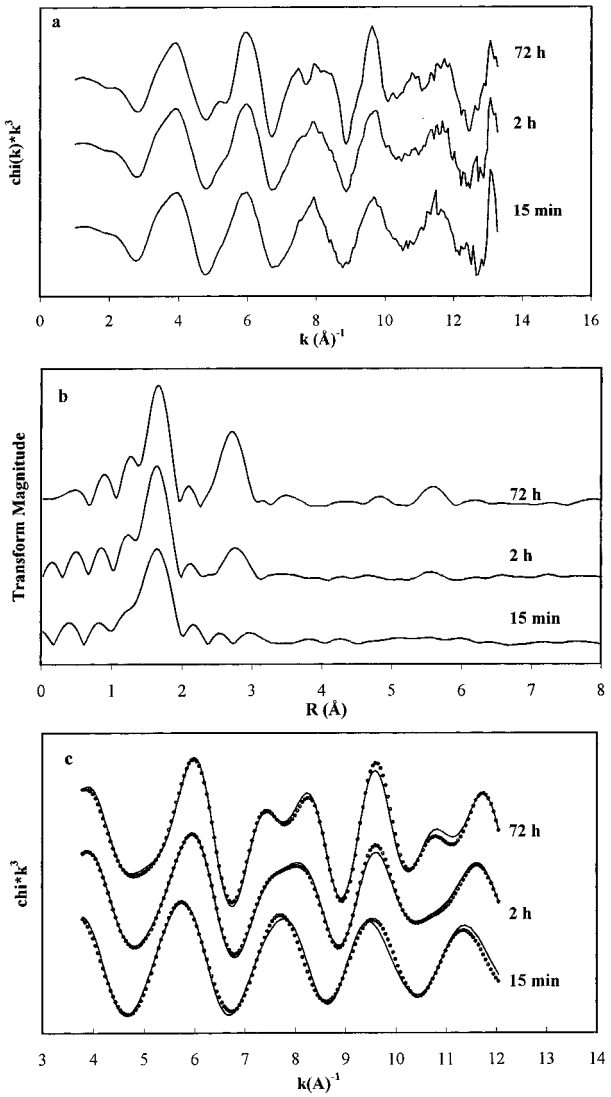

FIGURE 3. Results of EXAFS experiments performed at pH 6.8. (a) k^3-weighted, normalized, background-subtracted χ functions for Ni sorbed on soil clay for different times. (b) Fourier transforms of χ functions in panel a, uncorrected for phase shift. (c) Experimental k^3-weighted XAFS data (solid line) of Fourier back-transformed spectra in comparison to theoretical spectra (dotted line) using multi-shell least-squares fitting.

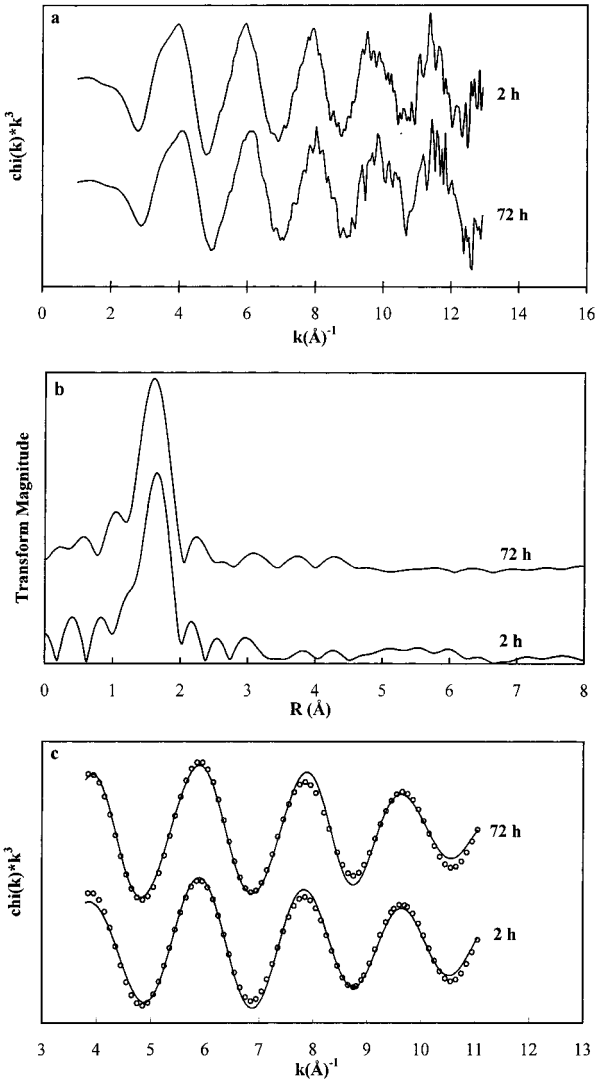

FIGURE 4. Results of EXAFS experiments performed at pH 6.0. (a) k^3-weighted, normalized, background-subtracted χ functions for Ni sorbed on soil clay for different times. (b) Fourier transforms of χ functions in panel a, uncorrected for phase shift. (c) Experimental k^3-weighted XAFS data (solid line) of Fourier back-transformed spectra in comparison to theoretical spectra (dotted line) using single-shell least-squares fitting.

72 h), a beat pattern developed within the XAFS spectra indicating multiple frequencies from second shell backscattering. The radial structure functions (uncorrected for phase shift) are shown in Figure 3b. Similar to the pH 7.5 system, the first peak at $R \cong 1.7$ Å remains relatively constant in amplitude with increasing reaction time. The second peak at $R \cong 2.8$ Å does not appear until after 2 h of reaction time. Similar to the pH 7.5 system, this second shell peak increases in magnitude over time.

Comparison of the k^3-weighted XAFS functions for the Fourier back-transformed spectra to the theoretical spectra derived by fitting theoretical Ni−O, Ni−Ni, and Ni−Al scattering paths to the raw data is shown in Figure 3c. The comparison indicates that the theoretical paths provide a good representation of the experimental data. The structural parameters derived from the fits are presented in Table 1. For the 15-min sample, a multi-shell fit was not reasonable since there was no higher RSF peak and it did not improve the fit quality. Analysis shows the same results for the Ni−O shell as was found in the pH 7.5 system for all samples. For the 2- and 72-h samples, the Ni−Ni and Ni−Al shell results were similar to the pH 7.5 system. The reduced Ni−Ni bond distance compared to α-$Ni(OH)_2$ suggests that the formation of a mixed Ni−Al LDH may be occurring within 2 h at this pH.

XAFS Analyses of Ni-Reacted Clay at pH 6.0. The k^3-weighted, normalized, background-subtracted χ functions for Ni sorbed on the soil clay at pH 6.0 for 2 and 72 h are presented in Figure 4a. The simple single oscillation of the XAFS signal remains relatively constant over time, indicating no contribution from a heavy backscattering element. The RSFs are presented in Figure 4b and are uncorrected for phase shift. As for the pH 7.5 and pH 6.8 systems, the Ni−O peak at $R \cong 1.7$ Å is observed and remains constant with increasing reaction time. In contrast to the pH 7.5 and pH 6.8 systems, no peak is present at $R \cong 2.8$ Å in any of the spectra, indicating that no second neighbor Ni atoms are present. This indicates that at this pH there is no formation of a precipitate within 72 h. Since there is little additional sorption of Ni after 72 h (Figure 1b), we do not anticipate the formation of precipitates after longer times. For this reason, the data were fit with only a Ni−O shell. The comparison of

the k^3-weighted XAFS functions for the Fourier back-transformed spectra to the theoretical spectra derived with parameters from analysis of a single shell are presented in Figure 4c. The comparison indicates good agreement between theoretical and experimental data. The structural parameters are presented in Table 1. XAFS data analysis indicated that Ni was in octahedral coordination with O with $N_{Ni-O} \cong 6$ and $R_{Ni-O} \cong 2.05$ Å (Table 1).

The results from the pH 6.0 system indicate that only adsorption phenomena are occurring for reaction times up to 72 h. Due to the heterogeneous nature of this soil clay, it is likely that both planar permanent-charge sites and edge surface-hydroxyl sites are competing for Ni sorption. The absence of precipitates at this low pH may be due to a pH effect and/or a surface-loading effect. Results from other studies investigating mixed-metal precipitate formation on clay minerals and oxides suggested that precipitate formation was dependent on the amount of metal ions sorbed to the surface at a given pH (*16*, *19*, *27*). Another explanation may be that a certain pH value must be attained prior to the formation of a metal precipitate phase, regardless of surface loading, to satisfy solubility requirements. The pH 6.0 system possibly needed more time to react with the soil clay prior to the formation of a precipitate. Figure 1b suggests, however, that even at longer times no precipitate will form since additional Ni uptake after 72 h is only minor.

Acknowledgments

The authors appreciate the support of this research by the USDA (NRICGP), the DuPont Co., the State of Delaware, and the NSF. D.R.R. appreciates the support of a Graduate Fellowship from the NSF. Thanks to Eef Elzinga and Drs. Andreas Scheinost and Robert Ford for their thorough reviews and suggestions.

Literature Cited

(1) Forstner, U. In *Metal Speciation and Contamination of Soil*; Allen, H. E., Huang, C. P., Bailey, G. W., Eds.; CRC Press: Boca Raton, FL, 1995.
(2) Mattigod, S. V.; Gibali, A. S.; Page, A. L. *Clays Clay Miner.* **1979**, *27*, 411−416.
(3) Tiller, K. G.; Gerth, J.; Brummer, G. *Geoderma* **1984**, *34*, 1−16.
(4) Ziper, C.; Komarneni, S.; Baker, D. E. *Soil Sci. Soc. Am. J.* **1988**, *52*, 49−53.
(5) Bruemmer, G. W.; Gerth, J.; Tiller, K. G. *J. Soil Sci.* **1988**, *39*, 37−52.
(6) Puls, R. W.; Powell, R. M.; Clark, D.; Eldred, C. J. *Water Air Soil Pollut.* **1991**, *57*−*58*, 423−430.
(7) Sparks, D. L. *Environmental Soil Chemistry*; Academic Press: San Diego, 1995.
(8) Brown, G. E., Jr.; Parks, G. A.; O'Day, P. A. In *Mineral Surfaces*; Vaughan, D. J., Pattrick, R. A. D., Eds.; Chapman & Hall: London, 1995; pp 129−183.
(9) Bertsch, P. M.; Hunter, D. B. In *Future of Soil Chemistry*; Huang, P. M., Sparks, D. L., Boyd, S. A., Eds.; SSSA: Madison, WI, 1999.
(10) Chisholm-Brause, C. J.; O'Day, P. A.; Brown, G. E., Jr.; Parks, G. A. *Nature* **1990**, *348*, 528−531.
(11) Charlet, L.; Manceau, A. A. *J. Colloid Interface Sci.* **1992**, *148*, 443−458.
(12) Spadini, L.; Manceau, A.; Schindler, P. W.; Charlet, L. *J. Colloid Interface Sci.* **1994**, *168*, 73−86.
(13) Charlet, L.; Manceau, A. *Geochim. Cosmoshim. Acta* **1994**, *58*, 2577−2582.
(14) O'Day, P. A.; Brown, G. E., Jr.; Parks, G. A. *J. Colloid Interface Sci.* **1994**, *165*, 269−289.
(15) Papelis, C.; Hayes, K. F. *Colloids Surf. A* **1996**, *107*, 89−96.
(16) O'Day, P. A.; Chisholm-Brause, C. J.; Towle, S. N.; Parks, G. A.; Brown, G. E., Jr. *Geochim. Cosmoshim. Acta* **1996**, *60*, 2515−2532.
(17) Bargar, J. R.; Brown, G. E., Jr.; Parks, G. A. *Geochim. Cosmoshim. Acta* **1997**, *61*, 2617−2637.
(18) Bargar, J. R.; Brown, G. E., Jr.; Parks, G. A. *Geochim. Cosmoshim. Acta* **1997**, *61*, 2639−2652.
(19) Towle, S. N.; Bargar, J. R.; Brown, G. E., Jr.; Parks, G. E. *J. Colloid Interface Sci.* **1997**, *187*, 62−82.
(20) Scheidegger, A. M.; Strawn, D. G.; Lamble, G. M.; Sparks, D. L. *Geochim. Cosmochim. Acta* **1998**, *62*, 2233−2245.
(21) Pickering, I. J.; Brown, G. E., Jr.; Tokunaga, T. K. *Environ. Sci. Technol.* **1995**, *29*, 2457−2459.
(22) Manceau, A.; Boisset, M. C.; Sarbet, G.; Hazemann, J.; Mench, M.; Cambier, P.; Prost, R. *Environ. Sci. Technol.* **1996**, *30*, 1540−1552.
(23) Morris, D. E.; Allen, P. G.; Berg, J. M.; Chisholm-Brause, C. J.; Conradson, S. D.; Donohoe, R. J.; Hess, N. J.; Musgrave, J. A.; Tait, C. D. *Environ. Sci. Technol.* **1996**, *30*, 2322−2331.
(24) O'Day, P. A.; Carroll, S. A.; Waychunas, G. A. *Environ. Sci. Technol.* **1998**, *32*, 943−955.
(25) Fendorf, S. E.; Lamble, G. M.; Stapleton, M. G.; Kelley, M. J.; Sparks, D. L. *Environ. Sci. Technol.* **1994**, *28*, 284−289.
(26) d'Espinose de la Caillerie, J.-B.; Kermarec, M.; Clause, O. *J. Am. Chem. Soc.* **1995**, *117*, 11471−11481.
(27) Scheidegger, A. M.; Lamble, G. M.; Sparks, D. L. *Environ. Sci. Technol.* **1996**, *30*, 548−554.
(28) Weesner, F. J.; Bleam, W. F. *J. Colloid Interface Sci.* **1997**, *196*, 79−86.
(29) Xia, K.; Mehadi, A.; Taylor, R. W.; Bleam, W. F. *J. Colloid Interface Sci.* **1997**, *185*, 252−257.
(30) Scheinost, A. C.; Ford, R. G.; Sparks, D. L. *Geochim. Cosmochim. Acta* **1999**, *63*, In press.
(31) Sparks, D. L. *Kinetics of Soil Chemical Processes*; Academic Press: San Diego, 1989.
(32) Lavkulich, L. M.; Wiens, J. H. *Soil Sci. Soc. Am. Proc.* **1970**, *34*, 755−758.
(33) Mehra, O. P.; Jackson, M. L. *Clays Clay Miner.* **1960**, *7*, 317−327.
(34) Moore, D. M.; Reynolds, R. C. *X-ray Diffraction and the Identification and Analysis of Clay Minerals*; Oxford University Press: New York, 1989.
(35) Karanthanasis, A. D.; Harris, W. G. In *Quantitative Methods in Soil Mineralogy*; Amonette, J. E., Zelazny, L. W., Eds.; SSSA, Inc.: Madison, WI, 1994; pp 360−411.
(36) Carter, D. L.; Mortland, M. M.; Kemper, W. D. In *Methods of Soil Analysis Part 1*−*Physical and Mineralogical Methods*, 2nd ed.; Klute, A., Ed.; ASA, Inc.: Madison, WI, 1986; pp 413−422.
(37) Jackson, M. L. Soil Chemical Analysis−Advanced Course, University of Wisconsin, 1956.
(38) Mattigod, S. V.; Rai, D.; Felmy, A. R.; Rao, L. *J. Solution Chem.* **1997**, *26*, 391−403.
(39) Thompson, H. A. Ph.D. Dissertation, Stanford University, CA, 1998.
(40) Lytle, F. W.; Greegor, R. B.; Sandstorm, D. R.; Marques, E. C.; Wong, J.; Spiro, C. L.; Huffman, G. P.; Huggins, F. E. *Nucl. Instrum. Methods* **1984**, 542−548.
(41) Bouldin, C.; Elam, T.; Furenlid, L. *Physica B* **1995**, *208/209*, 190−192.
(42) Boyanov, B. XFTools Collection, North Carolina State University, 1997, unpublished.
(43) Zabinsky, S. L.; Rehr, J. J.; Ankudinov, A.; Albers, R. C.; Eller, M. J. *Phys. Rev. B* **1995**, *52*, 2995−3006.
(44) Greaves, C.; Thomas, M. A. *Acta Crystallogr.* **1986**, *B42*, 51−55.
(45) Strawn, D. G.; Scheidegger, A. M.; Sparks, D. L. *Environ. Sci. Technol.* **1998**, *32*, 2596−2601.
(46) O'Day, P. A.; Rehr, J. J.; Zabinsky, S. I.; Brown, G. E., Jr. *J. Am. Chem. Soc.* **1994**, *116*, 2938−2949.
(47) Scheinost, A. C.; Sparks, D. L. *J. Colloid Interface Sci.*, In review.

Received for review March 1, 1999. Revised manuscript received August 16, 1999. Accepted August 23, 1999.

ES990235E